Fast hybrid method for analyzing the Doppler spectral of a moving plasma-coated target above a time-evolving lossy dielectric sea surface

Rui Wang*[1], Shui-rong Chai[1], and Li-xin Guo[1]

[1] Xidian University, 2 South Taibai Road, Xi'an Shaanxi, China, doufuruier@xidian.edu.cn

Abstract

A fast hybrid method that combines the reciprocity theorem with high frequency approximation algorithm is proposed to analyze the Doppler spectral from a two-dimensional moving plasma-coated object above a one-dimensional time-evolving lossy dielectric sea rough surface. This hybrid method eliminates the need for numerical solution of the polarization currents on object and time-evolving sea surface, thereby saving the computer resources and greatly improving the computing speed when compared to the conventional numerical methods. The characteristics of Doppler spectrum from a plasma-coated object above a time-evolving sea surface are analyzed in detail.

1. Introduction

Electromagnetic (EM) wave scattering from the sea surface has been intensively studied, for now more than half a century. To take benefit from the fluid motion and get much more information than radar cross-section, one can perform a coherent integration in time with a Doppler radar. Thus, the Doppler spectrum of the time-evolving sea surfaces has received considerable attention and studied both experimentally and theoretically for the past several decades [1-5]. These works mentioned above are focused on the Doppler spectrum of the sea surface only. However, the Doppler spectral analysis for a moving object above a time-evolving sea surface should be attracted much interest because the issue is of obvious interest in problems of object detection over the sea rough surface. As well as we know, the square modulus of the time Fourier transform of the complex backscattered field is called the Doppler spectrum. The time-dependent backscattered signals from a moving object and a time-evolving surface should be obtained to calculate the Doppler spectrum of the composite model. To get the Doppler spectrum of the composite model, it should be quite computationally expensive. This has formed the genesis for the research on more powerful strategies. In this paper, we have presented a fast hybrid strategy combining the reciprocity theorem with high frequency approximation algorithm, as a potential method to simulate the Doppler spectrum of the backscattering from a plasma-coated object above a dielectric rough surface. This method allows the use of physical optics (PO) for composite scattering problems, thereby improving the computing speed compared to the classical numerical methods, while still retaining certain accuracy under some conditions. The remainder of this paper is organized as follows. Section 3 is devoted to the EM scattering model of a plasma-coated object above a rough sea surface including the primary theoretical formulations of the hybrid method. In Section 4, we present the numerical results of the Doppler spectra of the backscattering from a plasma-coated object above a time-evolving sea surface are analyzed in detail. The paper ends with a section for concluding remarks and perspectives in this topic.

2. Scattering and Doppler Spectrum Calculation

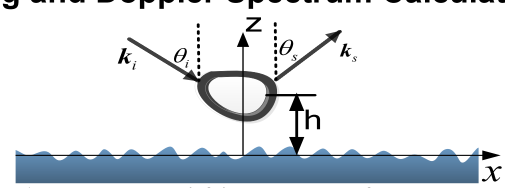

Fig. 1 Plasma-coated airfoil over a sea surface

The basic geometry of EM scattering from a plasma-coated object with coating thickness   above a 1D sea surface is shown in Fig. 1, wherein the plasma-coated object is positioned at the height of *h*. The sea surface profiles used in the study are realizations of a random process in PM spectrum. Fig. 2 illustrates the scattering mechanisms considered in the multipath model. Path (a) and (b) denote monostatic scattering path for the direct backscattered field from rough interface and object, respectively. Path (c) represents the second-order (2nd order) backscattered field, known as the "surface-object" backscattering. Similarly, Path (d) also corresponds to the second order backscattered field, known as the "object-surface" backscattering. Path (e) and Path (f) correspond to the third order backscattered fields, namely, "surface-object-surface" and "object-surface-object" backscattering. Accordingly, the total backscattered field can be written as follows:

$$\boldsymbol{E} = \boldsymbol{E}_1 + \boldsymbol{E}_2 + \boldsymbol{E}_{12} + \boldsymbol{E}_{21} + \boldsymbol{E}_{121} + \boldsymbol{E}_{212} \tag{1}$$

978-1-4673-5225-3/14/$31.00 ©2014 IEEE

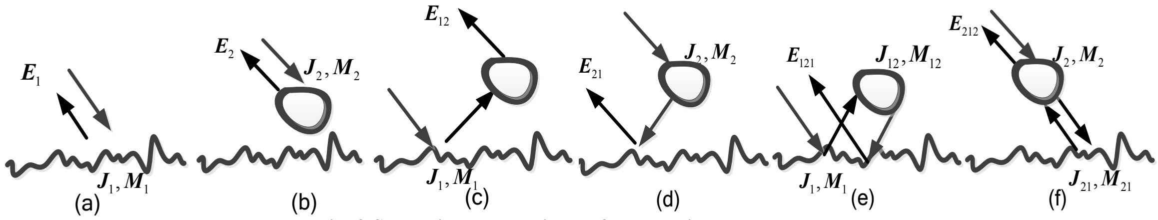

Fig. 2 Scattering mechanisms of the multipath model

here $\boldsymbol{E}_1$ and $\boldsymbol{E}_2$ can be obtained by PO, respectively. In this paper, the reciprocity theorem is employed to evaluate the rescattered coupling interaction between the plasma-coated object and the rough surface. When the object is illuminated by $\boldsymbol{J}_e$, as shown in Fig. 3(a), the corresponding scattered fields of $\boldsymbol{J}_{e2}$ and $\boldsymbol{M}_{e2}$ can be denoted as $\boldsymbol{E}_{Je2} = \boldsymbol{E}_{Je21} + \boldsymbol{E}_{Me21}$. When the object is illuminated by $\boldsymbol{M}_m$, shown in Fig. 3(b), the corresponding scattered fields of $\boldsymbol{J}_{m2}$ and $\boldsymbol{M}_{m2}$ can be denoted as $\boldsymbol{H}_{Mm2}(\boldsymbol{\rho}_s) = \boldsymbol{H}_{Jm21}(\boldsymbol{\rho}_s) + \boldsymbol{H}_{Mm21}(\boldsymbol{\rho}_s)$.

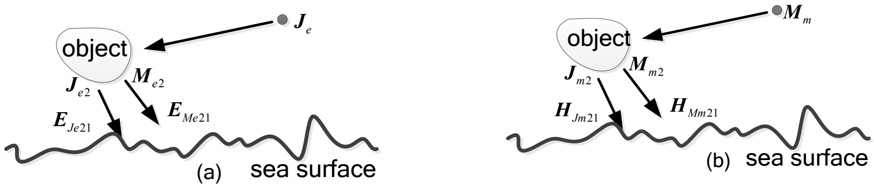

Fig. 3 Scattered fields of the object illuminated by $\boldsymbol{J}_e$ and $\boldsymbol{M}_m$

According to the reciprocity theorem [6-7]

$$\hat{\boldsymbol{y}} \cdot \boldsymbol{E}_{J12} = \int_s \boldsymbol{J}_1 \cdot \boldsymbol{E}_{Je2} ds \tag{2}$$

$$\hat{\boldsymbol{q}} \cdot \boldsymbol{H}_{M12} = \int_s \boldsymbol{M}_1 \cdot \boldsymbol{H}_{Mm2} ds \tag{3}$$

The "surface-object" backscattered fields $\boldsymbol{E}_{12} = \boldsymbol{E}_{J12} + \boldsymbol{E}_{M12}$ (shown in Fig. 2(c)) can be obtained using the relation $\boldsymbol{E}_{M12} = -\eta_0 \hat{\boldsymbol{k}}_s \times \boldsymbol{H}_{M12}$. Path (c) and (d) shown in Fig. 2 are identical under time reversal, which implies that the second-order monostatic scattered field can be expressed as $2 \times \boldsymbol{E}_{12}$. Considering the scattered field of $\boldsymbol{E}_i$ from underlying rough surface as the incident field to illuminate the coated object, we can evaluate the equivalent surface electric and magnetic currents densities $\boldsymbol{J}_{12}$ and $\boldsymbol{M}_{12}$ on the object by using PO. Based on the reciprocity theorem,

$$\hat{\boldsymbol{y}} \cdot \boldsymbol{E}_{J121} = \int_c \boldsymbol{J}_{12} \cdot \boldsymbol{E}_{Je1} dc \tag{4}$$

$$\hat{\boldsymbol{q}} \cdot \boldsymbol{H}_{M121} = \int_c \boldsymbol{M}_{12} \cdot \boldsymbol{H}_{Mm1} dc \tag{5}$$

By using this technique, we obtain the third order monostatic scattering $\boldsymbol{E}_{121}$, which can be obtained as $\boldsymbol{E}_{121} = \boldsymbol{E}_{J121} + \boldsymbol{E}_{M121}$, where the relation $\boldsymbol{E}_{M121} = -\eta_0 \hat{\boldsymbol{k}}_s \times \boldsymbol{H}_{M121}$ has been used. Similarly, considering the scattered field of $\boldsymbol{E}_i$ from the coated object as the incident field to illuminate the underlying rough surface, we can evaluate the equivalent surface electric and magnetic currents densities $\boldsymbol{J}_{21}$ and $\boldsymbol{M}_{21}$ on the rough surface by using PO. Based on the reciprocity theorem, we have

$$\hat{\boldsymbol{y}} \cdot \boldsymbol{E}_{J212} = \int_s \boldsymbol{J}_{21} \cdot \boldsymbol{E}_{Je2} ds \tag{6}$$

$$\hat{\boldsymbol{q}} \cdot \boldsymbol{H}_{M212} = \int_s \boldsymbol{M}_{21} \cdot \boldsymbol{H}_{Mm2} ds \tag{7}$$

Accordingly, the "object-surface-object" coupling the backscattered fields $\boldsymbol{E}_{212}$ shown in Fig. 2(f)) can be obtained as $\boldsymbol{E}_{212} = \boldsymbol{E}_{J212} + \boldsymbol{E}_{M212}$. The total scattered field of the composite model can be written as follows:

$$\boldsymbol{E} = \boldsymbol{E}_1 + \boldsymbol{E}_2 + 2 \times \boldsymbol{E}_{21} + \boldsymbol{E}_{121} + \boldsymbol{E}_{212} \tag{8}$$

The Doppler spectrum is a power spectral density of the random time-varying complex amplitude of the backscattered field. To evaluate it, we used a standard spectral estimation technique. Thus, the expression of the Doppler spectrum may be defined as [1]

$$S_0(f) = \frac{1}{T} \left| \int_0^T E(t, \theta_i, \theta_s) \exp(-j2\pi f t) dt \right|^2 \tag{9}$$

and in the case of backscattering, we have $\theta_s = -\theta_i$. The final Doppler spectrum can be calculated as the average

$$S(f)=\frac{1}{M}\sum_{m=1}^{M}S_0^m(f) \tag{10}$$

where $S_0^m(f)$ is the single realization of the Doppler spectrum obtained by (9).

3. Numerical results

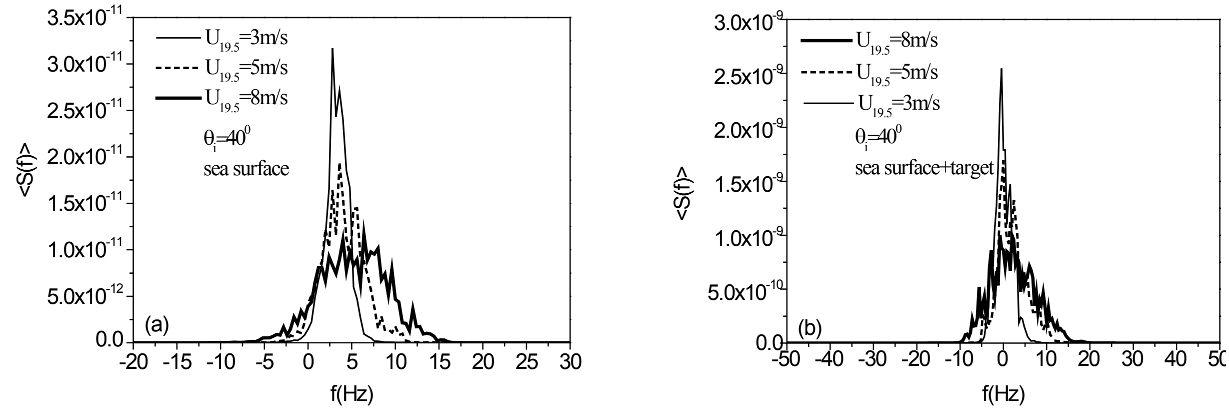

Fig. 4. The Doppler spectrum of the backscattered field for different wind speeds.

Fig. 4 (a) gives us the Doppler spectrum of the backscattered field from the sea surface only with different wind speeds. We can find that with increasing the wind speed, the velocities of the surface water and the orbital motion for the sea wave with large-scale increase, for the Doppler spectrum of the backscattering from the sea surface, there has been a gradual increase for the Doppler spectrum frequency shift, which is coincident with the measuring results by Rozenberg *et al* [8]. On the other hand, there also exists a broadening for the lobe of the Doppler spectrum with the wind speed increasing. This phenomenon is mainly due to the fact that the incoherent scattering increases with the increase in the roughness of the sea surface, and thus the backscattering energy will be distributed over a wide region of the frequency domain, which has been discussed in [5, 9-10]. Unlike Fig. 4(a), there is nearly no increase for the Doppler spectrum frequency shift. The main reason may be the existence of the deterministic object, which results in the "roughness" of the composite model decrease and whereupon, there is the decrease of the incoherent scattering. Moreover, all the maximum value of spectral density of the Doppler spectrum for the composite model and the surface only become small with the increase of windspeed.

Fig.5, the Doppler spectrum of the total backscattering from the composite model is presented with the different incident angles. It is clear that two main Doppler spectrum lobes appear obviously over the spectral domain for each incident angle. One of the Doppler spectrum lobes is mainly concerned with the backscattering from the sea surface only. The other is not only concerned with the backscattering from the moving object only but also the coupling backscattering between sea surface and moving object especially at big incident angle. It is found that the two spectral lobes move away from each other as the incident angle increases due to the moving of the object. This is of great importance for the object detection above the sea surface especially for the low grazing angles. Fig.6 shows the relationship between the Doppler spectrum of the total backscattered field and the velocity of the object. It can be seen that the frequency shift of the first main Doppler spectrum lobe does not change with the different velocity of the moving object, while the frequency shift of the second main Doppler spectrum lobe is in directly proportional to the velocity of the moving object.

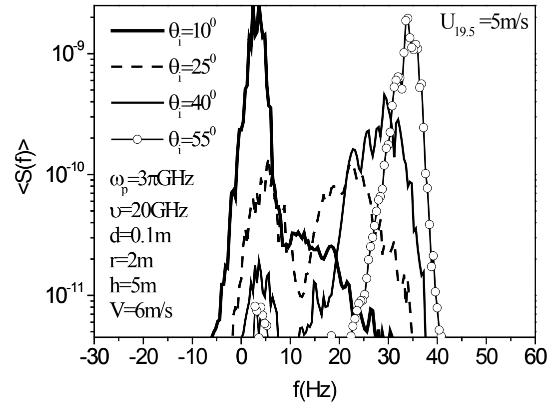

Fig. 5. The Doppler spectrum of the backscattering from composite model for different incident angles

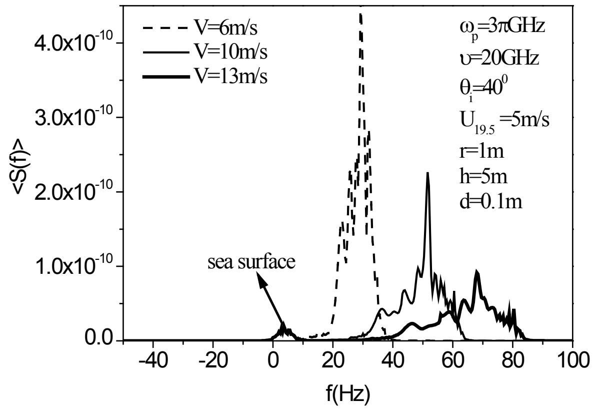

Fig. 6. The Doppler spectrum of the total backscattering from composite model for different velocity of the moving object

In Fig. 7(a), we investigated the dependence of the Doppler spectrum of the total backscattered field on the thickness of the plasma coating *d*. As is seen, the amplitude of the right-hand Doppler spectrum lobe decrease with increase in d and attain the minimum values near d=0.1m, indicating the best stealth effect. The amplitude for d=0.3m is the same as that for d=0.1m, which demonstrates that there is an optimum value of d. To consider the influence of plasma angular frequency on the Doppler spectrum, in Fig.7(b), we performed simulations to compare the amplitude of the Doppler spectrum for different values of plasma angular frequency. We can see that the change of plasma angular frequency has no influence on the left-hand lobe of the spectrum which is mainly concerned with the backscattering from the sea surface only. The amplitude of the right-hand Doppler spectrum lobe reach a minimal value at $6\pi\text{GHz}$. Thus, it can be concluded that there is still an optimum value of plasma frequency at given incidence and electron collision frequency. Plasma frequency higher or lower than this optimum frequency would lead to smaller amplitude reduction.

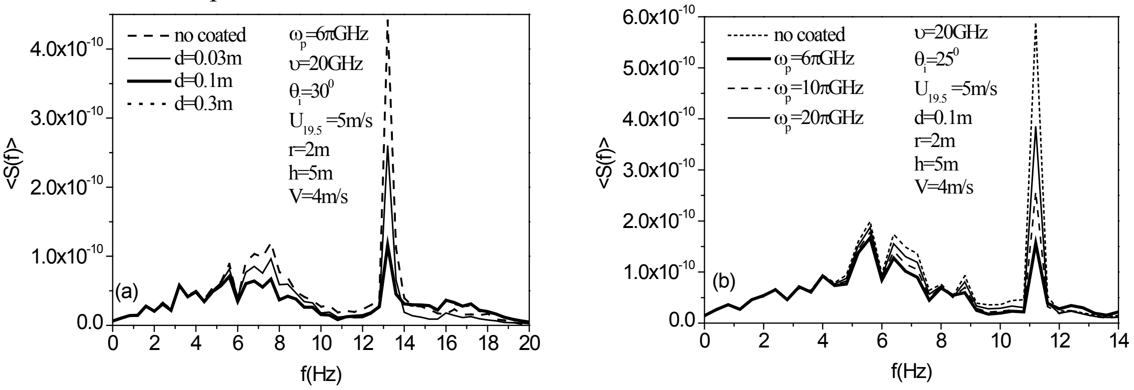

Fig. 7. The Doppler spectrum of the total backscattered field for different (a) thickness of the plasma coating (b) plasma angular frequency

4. Conclusion

In this paper, the Doppler spectral from a 2D moving plasma-coated object above a 1D time-evolving lossy dielectric sea rough surface is evaluated by using a fast hybrid method that combines the reciprocity theorem with high frequency approximation algorithm. The dependence of the Doppler spectrum of the composite field upon the wind speed, the incident angles, as well as the key parameters on stealth performance of the plasma-coated object are numerically demonstrated and discussed. For the numerical results, it can be seen that there is not a monotonic change of the Doppler spectrum peak with the increase of the thickness of the plasma coating (see Fig. 16) and the plasma angular frequency (see Fig. 17) which demonstrate the fact that there are some optimum values of the key plasma parameters at given condition and the key parameters higher or lower than optimum value would lead to smaller amplitude reduction.

5. Acknowledgments

This work was supported in part by the National Natural Science Foundation of China (Grant No. 61301070), by the National Natural Science Foundation for Distinguished Young Scholars of China (Grant No. 61225002) and by the Specialized Research Fund for the Doctoral Program of Higher Education (Grant 20120203120023).

6. References

1. J. V. Toporkov and G. S. Brown, "Numerical simulations of scattering from time-varying randomly rough surfaces," *IEEE Trans. Geosci. Re-mote Sens.*, 38(4), pp. 1616–1625, Jul. 2000.
2. G. Soriano, M. Joelson, M. Saillard, and P. C. Marseille, "Doppler spectra from a two-dimensional ocean surface at L-band," *IEEE Trans. Geosci. Remote Sens.*, 44(9), pp. 2430–2437, Sep. 2006.
3. Yunhua Wang, Yanmin Zhang, Mingxia He, and Chaofang Zhao, "Doppler Spectra of Microwave Scattering Fields From Nonlinear Oceanic Surface at Moderate- and Low-Grazing Angles" *IEEE Trans. Geosci. Remote Sens.,* 50(4), pp. 1104-1116, Apr.. 2012.
4. Xiaofei Li ; Xiaojian Xu, "Scattering and Doppler Spectral Analysis for Two-Dimensional Linear and Nonlinear Sea Surfaces ", *IEEE Trans. Geosci. Remote Sens.*, 49(2), pp. 603-611, Feb. 2011.
5. J. T. Johnson, J. V. Toporkov, and G. S. Brown, "A numerical study of backscattering from time-evolving sea surfaces: Comparison of hydro-dynamic models," *IEEE Trans. Geosci. Remote Sens.*, 39(11), pp. 2411–2420, Nov. 2001.
6. J. A. Kong, Electromagnetic wave theory, *Wiley-Interscience*, 2002.
7. Y. H. Wang, L. X. Guo, Z. S. Wu, Electromagnetic scattering of Gaussian beam by 2-D targets, *Radio Science*, 42(4): RS4012, 2007.
8. A. D. Rozenberg, D. C. Quigley, and W. K. Melville, "Laboratory study of polarized micro-wave scattering by surface waves at grazing incidence: part I-wind waves", *IEEE Trans. Geosci. Remote Sens*. 33, pp. 1037–1046, 1995.
9. J. V. Toporkov and G. S. Brown, "Numerical study of the extended Kirchhoff approach and the lowest order small slope approximation for scattering from ocean-like surfaces: Doppler analysis," *IEEE Trans. Antennas Propag.* 50, pp. 417–425 (2002).
10. L. X. Guo, Y. H. Wang, and Z. S. Wu, " Study on the electromagnetic scattering and Doppler spectra from two-scale time-varying fractal rough sea surface," *Acta Phys. Sin.* 54, pp. 96–101, 2005.